Determination of Degree of Crosslinking in Natural Rubber Vulcanizates. Part IV. Stress–Strain Behavior at Large Extensions

L. MULLINS

British Rubber Producers' Research Association, Welwyn Garden City, Herts., England

1. INTRODUCTION

The statistical theory of rubberlike elasticity predicts that the stress–strain behavior of vulcanized rubber in simple extension is given by

$$f = A_0 \nu kT(\lambda - \lambda^{-2}) \qquad (1)$$

where f is the force required to extend a sample of rubber with a density of ν network chains per unit volume to an extension ratio λ, and where k is Boltzmann's constant, T the absolute temperature, and A_0 the unstrained cross-sectional area.

Appreciable deviations from the predictions of the statistical theory occur at low and moderate extensions, and a considerably better description of experimental stress–strain behavior can be obtained by the use of the first approximation of a generalized theory of large elastic deformations developed by Rivlin.[1]

For simple extension, this gives

$$f = 2A_0(\lambda - \lambda^{-2})(C_1 + \lambda^{-1}C_2) \qquad (2)$$

The contribution of the term involving C_1 to the force required to extend rubber has been identified with that predicted by the statistical theory[2,3]; thus,

$$C_1 = \frac{1}{2}\nu kT$$

or, alternatively:

$$C_1 = \frac{1}{2}\rho RTM_c^{-1}$$

where ρ is the density of the rubber, M_c the number-average molecular weight of the chain segments of rubber between adjacent crosslinks, and R is the gas constant.

Further deviations from the predictions of eqs. (1) and (2) occur at high extensions, and the value of the stress increases much more rapidly than predicted. Flory[4] and Wood[5] have associated this rapid upturn of the stress–strain curves with crystallization induced by molecular orientation at high strains. Treloar,[6] Kuhn and his associates,[7,8] Isihara, Hashitsume, and Tatibana,[9] and Wang and Guth[10] have shown that deviations of this type result naturally from the finite extensibility of network chain segments. At large strains, the use of the Gaussian distribution of chain-segment displacement lengths which was adopted in the derivation of eq. (1) becomes increasingly inadequate and quite unacceptable when the displacement lengths approach the full, extended length of the chain segments. This deficiency of the statistical theory has been dealt with by the introduction of more suitable distributions.[6,9,10]

The quantitative applications of this non-Gaussian statistical theory to stress–strain curves at high extensions has been hampered by inadequacies in methods of determining the network structure. Recent developments in characterization of network structure[3] now provide a possibility of quantitatively describing the onset of departures due to finite extensibility; these developments are examined in this paper.

2. APPLICATION OF NON-GAUSSIAN THEORY TO STRESS–STRAIN BEHAVIOR IN SIMPLE EXTENSION

Treloar[6] gives a modified stress–strain relationship for simple extension in a series expression the first four terms of which are:

$$f = A_0 \nu kT(\lambda - \lambda^{-2})\left[1 + \frac{3n^{-1}}{25}(3\lambda^2 + 4\lambda^{-1})\right.$$
$$+ \frac{297n^{-2}}{6125}(5\lambda^4 + 8\lambda + 8\lambda^{-2})$$
$$\left. + \frac{12,312n^{-3}}{2,205,000}(35\lambda^6 + 60\lambda^3 + 72 + 64\lambda^{-3} + \ldots)\right]$$
$$(3)$$

The use of eq. (3) to calculate theoretical stress–strain curves is extremely laborious; also, the series

TABLE I

Conjugate Values of λ^* and n Which Give a $2^1/_2\%$ Increase in the Value of C_1 due to Finite Extensibility

n	50	100	150	200	250	300
λ^*	1.89	2.50	2.95	3.39	3.74	4.09

cannot be satisfactorily approximated, since it approaches infinity as the chain segments become fully extended. However, its validity in regions where departures due to finite extensibility are small can be readily examined, as in these circumstances the contribution of higher terms in the polynomial becomes vanishingly small.

Departures from the predictions of the simple Gaussian theory, which are given by eq. (1), are described by a function of λ and n; thus, to describe their onset, a relationship between λ^*, the extension at which departures due to finite extensibility give a small but significant correction, and n was derived. An arbitrary value of $2^1/_2\%$ was chosen for the correction, and it was found that for the rubbers used in this investigation it was then sufficient to consider only the first three terms of the polynomial.

Values of the first three terms in the polynomial, *viz.*,

$$1 + (^3/_{25})n^{-1}(3\lambda^2 + 4\lambda^{-1})$$
$$+ (^{297}/_{6125})n^{-2}(5\lambda^4 + 8\lambda + 8\lambda^{-2})$$

were calculated for values of λ between 1.0 and 4.0 for selected values of n between 50 and 300, with the use of intervals of 0.2 between the values of λ and of 50 between the values of n. For each selected value of n, the ratio of the value of the expression to its value at $\lambda = 1$ was determined and conjugate values of λ^* and n, giving a ratio of
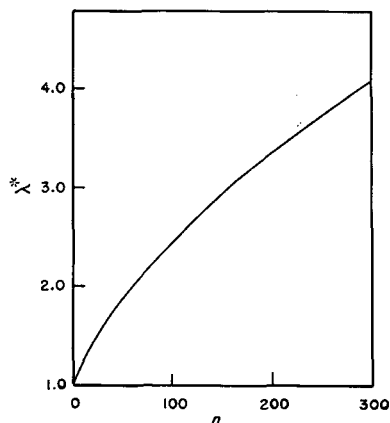
1.025 (an increase of $2^1/_2\%$), were obtained graphically. These are given in Table I, and shown in Figure 1.

3. STRESS–STRAIN BEHAVIOR AT LARGE EXTENSIONS

Experimental

Measurements were made of the equilibrium stress–strain properties in simple extension at 25°C., according to a procedure described previously.[2,3] A range of natural-rubber peroxide vulcanizates chosen to have as wide a range of initial molecular weights (Vulcanizates A-1 to A-5) and degree of crosslinking (Vulcanizates B-1 to B-5 and C-1 to C-5) as conveniently possible were examined. In addition, measurements were made on a range of natural-rubber accelerated sulfur vulcanizates. Full compounding details and vulcanizing procedures are given in the Appendix.

Values of the number-average initial molecular weight $\bar{M}_n$, were determined from measurements of the intrinsic viscosity of samples of the compounded stock applied to the limiting viscosity number–molecular weight relationship for masticated natural rubber recently established by Mullins and Watson:[15]

$$[\eta] = 2.29 \times 10^{-7}\bar{M}_n^{1.33} \qquad (4)$$

Stress–Strain Behavior of Dry Rubbers

Figures 2, 3, and 4 give results obtained on dry samples of peroxide vulcanized rubber. These are plotted as $^1/_2 fA_0^{-1}(\lambda - \lambda^{-2})^{-1}$ against λ^{-1}.
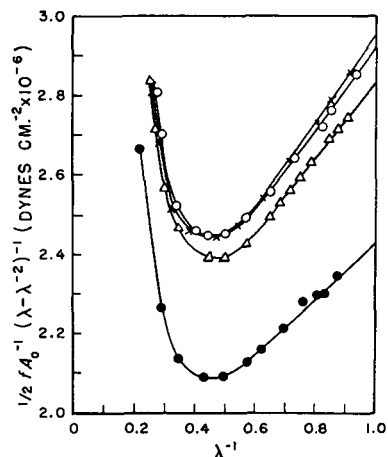
Fig. 1. Dependence of λ^* on chain segment length n.

Fig. 2. Dependence of stress–strain behavior on initial molecular weight: values of $\bar{M}_n^{-1} \times 10^6$ of ($\times$) 3.10; ($\bigcirc$) 3.95; ($\triangle$) 5.12; ($\bullet$) 7.05.
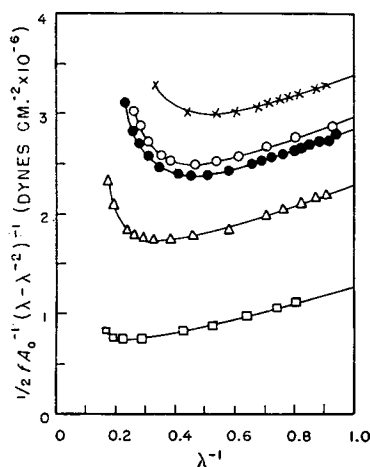
Fig. 3. Dependence of stress–strain behavior on period of vulcanization; (×) 160 min.; (○) 80 min.; (●) 60 min.; (△) 40 min.; (□) 10 min.

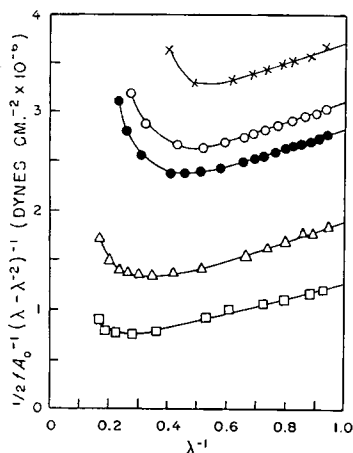Fig. 4. Dependence of stress–strain behavior on peroxide concentration: parts of peroxide per 100 parts rubber of (×) 5; (○) 4; (●) 3; (△) 2; (□) 1.

The figures show, respectively, the effect of initial molecular weight, of period of vulcanization, and of concentration of peroxide on the stress–strain behavior. All of the curves show that at low and moderate extensions there is a region where the stress–strain behavior can be described in terms of the two parameters C_1 and C_2. At higher extensions (smaller λ^{-1}), departures occur, and each curve goes through a minimum, the value of $\frac{1}{2}fA_0^{-1}$ $(\lambda - \lambda^{-2})^{-1}$ thereafter increasing rapidly with further extension.

Figure 2 shows that the value of λ^{-1} at which the minimum occurs is little affected by changes in initial molecular weight. However, Figures 3 and 4 show that the minimum occurs at larger values of λ^{-1} for more highly crosslinked rubbers.

Table II gives the values of C_1 and λ^*, the extension ratio at which the observed stress–strain curve departs from the linear portion by $2\frac{1}{2}\%$ of C_1, obtained from these curves.

TABLE II
Change in λ^* with Degree of Crosslinking
(Peroxide vulcanizates; density = 0.910 g./cm.³; measurements at 25 ± 0.2°C.)

Vulcani-zate	$\bar{M}_n^{-1} \times 10^6$	C_1, (dynes cm.$^{-2}$) $\times 10^{-6}$	λ^*	M_c (physical) $\times 10^{-3}$
A-1	3.10	1.85	2.04	5.72
2	3.95	1.90	2.06	5.51
3	5.12	1.86	2.06	5.49
4	7.05	1.67	2.17	5.73
5	9.65	1.57	2.10	5.71
B-1	5.12	0.56	2.95	10.75
2	5.12	1.27	2.28	7.41
3	5.12	1.86	2.06	5.49
4	5.12	1.93	2.04	5.31
5	5.12	2.35	1.82	4.46
C-1	5.12	0.57	3.10	10.76
2	5.12	1.04	2.25	8.40
3	5.12	1.86	2.06	5.49
4	5.12	2.06	2.00	5.02
5	5.12	2.57	1.82	4.08

In addition, it contains values of the reciprocal of the number-average initial molecular weight $\bar{M}_n$ obtained from intrinsic viscosity data together with estimates of the number-average molecular weight of chain segments between adjacent crosslinks. The values of the latter were obtained by use of an empirical correction for network flaws due to chain ends established previously[2,3] and given by the relation

$$C_1 = \frac{1}{2}\rho RT M_c^{-1} \text{ (physical)}$$

$$[1 - 2.3\, M_c \text{ (chemical)}\, M^{-1}] \quad (5)$$

where M_c^{-1} (physical) $= M_c^{-1}$(chemical) $+ 0.68 \times 10^{-4}$. Here the value of M_c(physical) is the effective number-average molecular weight of the network chain segments and includes the contribution of chemical crosslinks and chain entanglements. It thus describes the effective network which controls the behavior in finite extensibility considerations. The value of M_c(chemical) is the number-average molecular weight of chain segments bounded by chemical crosslinks at both ends.

Figure 5 shows the values of λ^* plotted against M_c(physical); the full curve in the figure was

TABLE III
Change in λ* with Degree of Crosslinking
(Sulfur vulcanizates; measurements at 25 ± 0.2°C.)

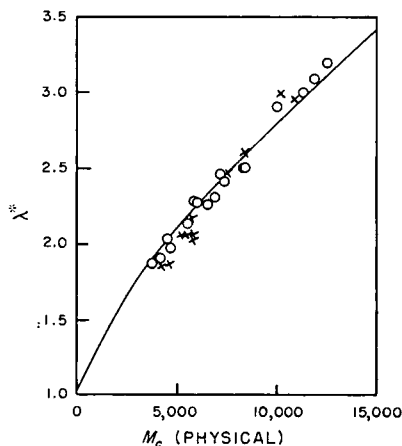| Vulcanizate	Density, g./cm.³	$M^{-1} \times 10^6$	C_1, (dynes-cm.$^{-2}$) $\times 10^{-6}$	λ*	M_c (physical) $\times 10^{-3}$
D-1	0.937	5.15	0.26	3.20	12.46
2		5.15	0.41	3.10	11.87
3		5.15	0.51	3.00	11.36
4		5.15	0.78	2.90	9.99
E-1	0.956	5.00	1.13	2.50	8.39
2		5.00	1.37	2.42	7.30
3		5.00	1.37	2.40	7.30
F-1	0.970	6.75	1.05	2.50	8.28
2		6.75	1.35	2.30	7.02
3		6.75	1.69	2.27	6.03
4		6.75	1.49	2.25	6.63
G-1	0.967	7.25	1.74	2.27	5.82
2		7.25	2.32	2.02	4.56
3		7.25	2.35	2.04	4.54
4		7.25	2.37	2.02	4.50
H-1	0.974	5.50	2.68	1.90	4.19
2		5.50	2.98	1.88	3.78
3		5.50	2.43	2.00	4.60

Fig. 5. Dependence of λ* on chain segment molecular weight of (O) peroxide vulcanizates; (X) sulfur vulcanizates.

plotted from the theoretical relation between λ* and n given in Figure 1 and fitted to the present data by the choice of an appropriate value for the molecular weight of the random link. It was found that a molecular weight of 75 for each link was required to obtain the fit shown in Figure 4 hence.

$$M_c = 75n \qquad (6)$$

Figure 5 also shows values of λ* and M_c(physical) obtained on a range of sulfur vulcanizates. The results are given in full in Table III.

Stress–Strain Behavior of Swollen Rubbers

In addition, measurements were made on one of the vulcanizates (A - 3) at different degrees of swelling. The results are given in Figure 6. These show the expected progressive reduction in the slope of the plot of $1/2 \; fA_0^{-1}(\lambda - \lambda^{-2})^{-1}v_r^{1/3}$ against λ^{-1} with increase in degree of swelling, but in addition they show that the extension at which the minimum and the following rapid upward sweep of the stress–strain curve occurs is less, the
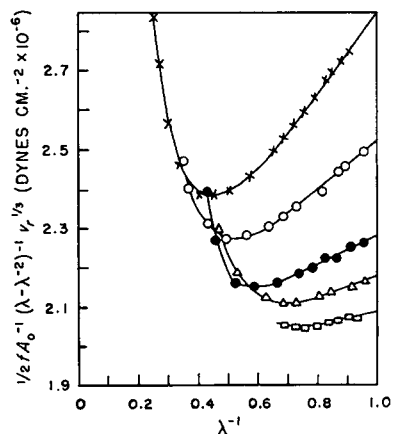

Fig. 6. Effect of swelling on stress–strain behavior: (X) $v_r = 1.000$; (O) $v_r = 0.753$; (●) $v_r = 0.585$; (△) $v_r = 0.455$; (□) $v_r = 0.407$.

higher the degree of swelling. Table IV gives the values of λ^* obtained from these curves for each degree of swelling.

The theoretical correction for finite extensibility leads to the prediction that the effect of swelling is equivalent to a reduction of the number of links n in the network chain segment to $nv_r^{2/3}$, where v_r is the volume fraction of rubber in the swollen vulcanizate. Table IV also includes values of $nv_r^{2/3}$, the value of n for this vulcanizate being determined by fitting the value of λ^* obtained on the dry vulcanizate on to the theoretical curve
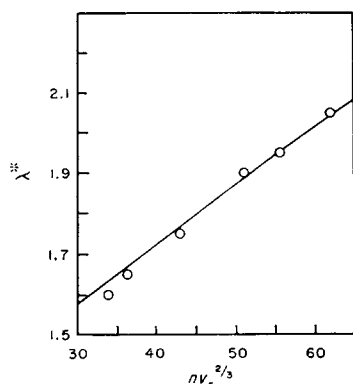

Fig. 7. Dependence of λ^* on degree of swelling.

relating λ^* and n given in Figure 1. (For this vulcanizate, it gave a molecular weight of 87 for a random link in the equivalent chain.)

The observed change in λ^* with $nv_r^{2/3}$ is shown in Figure 7. The full line in the figure is once again the theoretical curve given in Figure 1.

TABLE IV
Change in λ^* with Degree of Swelling
(Measurements at $25 \pm 0.2°C$. Vulcanizate A-3, density
0.910 g. cm.$^{-3}$, M_c(physical) = 5,490. Swelling medium,
n-decane.)

Volume swelling	λ^*	$nv_r^{2/3}$
1.000	2.06	63
0.855	1.95	55.7
0.753	1.90	51.2
0.585	1.75	43.3
0.455	1.65	36.5
0.375	1.60	34.0

The value of n of 63 for M_c (physical) of 5,490 corresponds to a molecular weight of the random link of 87.

5. DISCUSSION

The results of the dependence of λ^* on the degree of crosslinking which were given in Figure 5 show a most satisfactory agreement between the experimental determinations of the onset of departures which occur at large extensions, and theoretical predictions. They provide confirmation of the validity of the hypothesis that departures at high extensions are due to finite extensibility of the network and not to crystallization.

The results obtained on swollen rubbers which were given in Figure 6 provide further confirmation of the general validity of the treatment, and indicate that the effective network structure is the same in both the dry and swollen state.

In addition, the results provide an estimate of the size of the hypothetical random link, which is a basic parameter in the development of the statistical theory. The value of its molecular weight is not precisely determined, but a value of 75 ± 10 includes 90% of the experimental results and is equivalent to 1.1 ± 0.15 isoprene units; this is to be compared with a value of approximately 0.7 isoprene units obtained by Treloar[11] from theoretical calculations, approximate values of 1.5 isoprene units obtained by Treloar[12] and 2.2 isoprene units obtained by Saunders[13] from birefringence studies, and 2.8 isoprene units obtained by W. Kuhn and H. Kuhn[14] from viscosity data and flow birefringence. The most direct determinations are those by Treloar and Saunders and the one described here. Treloar and Saunders both used similar values of the stress-optical coefficient of rubber, and differences in their estimates of the size of a random link are due to differences in their calculated values of the optical anisotropy of a single isoprene unit. A measure of uncertainty of the correct value of this latter quantity still exists. The empirical estimate derived here, from a quite independent method of measurement and analysis, is in sufficiently close accord to justify the belief that the determination is on a sound basis.

The results lead to the two following important practical consequences.

Stress–Strain Behavior of Highly Swollen Rubbers

The curves on the effect of swelling on stress–strain behavior which were given in Figure 6 show that at high degrees of swelling departures due to finite extensibility occur at low elongations. As a
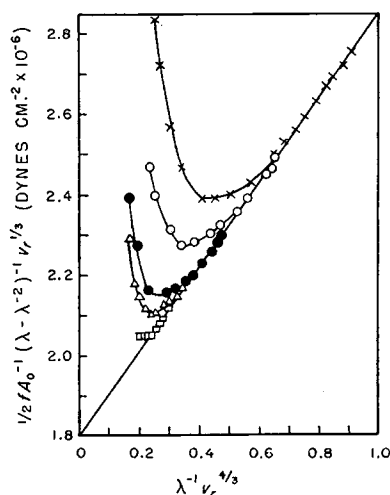
Fig. 8. Effect of swelling on C_1 and C_2. ($\times$) v_r = 1.000; (O) v_r = 0.753; ($\bullet$) v_r = 0.585; ($\triangle$) v_r = 0.455; ($\square$) v_r = 0.407.

result, the linear portions of the stress–strain curves which are used to determine C_1 and C_2 become very limited, and it appears that at very high degrees of swelling departures due to finite extensibility may already be present in swollen but unextended rubbers. This leads to difficulties in determining good estimates of C_1 and C_2 on highly swollen rubbers, and errors due to this cause will result in an increase in the estimated value of C_1 and a decrease in C_2.

However, it has been found that the experimental results of the dependence of C_1 and C_2 on degree of swelling can be described by the equation

$$\tfrac{1}{2} f A_0 (\lambda - \lambda^{-2})^{-1} v_r^{1/3}$$

$$= C_1(\text{dry}) v_r^{1/3} + \lambda^{-1} C_2(\text{dry}) v_r^{4/3} \quad (7)$$

and that a plot of $\tfrac{1}{2} f A_0 (\lambda - \lambda^{-2})^{-1} v_r^{1/3}$ against $\lambda^{-1} v_r^{4/3}$ gives a single straight line for all experimental data with an intercept on the ordinate of C_1 (dry). The data given in Figure 6 have been replotted in this way in Figure 8 and it will be seen that the two parameters C_1 and C_2 determined on the dry rubber characterize the behavior over the whole range of conditions apart from divergencies which occur at high extensions and high degrees of swelling. The source of both of these divergencies has already been attributed to finite extensibility and it now appears, contrary to previous suggestions,[2] that in the characterization of network structure, values of C_1 obtained on dry vulcanizates are preferred to values obtained on highly swollen vulcanizates.

Determination of Network Structure from Stress–Strain Measurements

The second practical consequence results from the recognition that the determination of C_1 and λ^* from a single simple extension stress–strain curve permits the calculation of *both* the degree of crosslinking and the initial molecular weight of the vulcanizate. The value of λ^* has been shown to reflect the degree of crosslinking and to be independent of initial molecular weight, while the value of C_1 reflects both the degree of crosslinking and network flaws due to chain ends. The determination of these two basic parameters describing network structures was hitherto unattainable from measurements on vulcanized rubbers alone. This development thus provides a new technique which is likely to be of particular value in studies of degradation occurring in vulcanized networks.

APPENDIX

Compounding details and vulcanization procedures were as follows.

Vulcanizates A-1–A-5

Smoked sheet 100, dicumyl peroxide 3 parts by weight. The compounded stock was divided into five equal parts which were masticated to give different degrees of breakdown. Vulcanization 60 min. at 140°C.

Vulcanizates B-1–B-5

Smoked sheet 100, dicumyl peroxide 3 parts by weight. Vulcanization 10, 40, 60, 80, and 160 minutes at 140°C., respectively.

Vulcanizates C-1–C-5

Smoked sheet 100, dicumyl peroxide 1, 2, 3, 4, and 5 parts by weight, respectively. Vulcanization 60 min. at 140°C.

Vulcanizates D-1–D-4

Smoked sheet 100, sulfur 5 parts by weight. Vulcanization 2, 3, 4, and 5 hr. at 140°C., respectively.

Vulcanizates E-1–E-3

Smoked sheet 100, sulfur 4, zinc oxide 5, stearic acid 1 parts by weight. Vulcanization 20, 40, and 60 min. at 140°C., respectively.

Vulcanizates F-1–F-4

Smoked sheet 100, tetramethylthiuram disulfide 6, zinc oxide 5, stearic acid 1 parts by weight. Vulcanization 10, 20, 30, and 40 min. at 140°C., respectively.

Vulcanizates G-1–G-4

Smoked sheet 100, sulfur 4, zinc oxide 5, stearic acid 1, N-cyclohexenylbenzthiazlsulfenamide 0.7 parts by weight. Vulcanization 10, 20, 30, and 40 min. at 140°C., respectively.

Vulcanizates H-1–H-3

Smoked sheet 100, sulfur 4, zinc oxide 5, stearic acid 1, mercaptobenzothiazole 0.5, diphenylguanidine 1 parts by weight. Vulcanization 15 and 17 min. at 140°C. and 4 hr. at 100°C., respectively.

References

1. R. S. Rivlin, *Phil. Trans. Roy. Soc., London, Ser. A,* **241,** 379 (1948).
2. L. Mullins, *J. Polymer Sci.,* **19,** 225 (1956).
3. L. Mullins, *J. Appl. Polymer Sci.,* **2,** 1 (1959).
4. P. J. Flory, *Ind. Eng. Chem.,* **38,** 417 (1946).
5. L. A. Wood, *J. Wash. Acad. Sci.,* **47,** 281 (1957).
6. L. R. G. Treloar, *Trans. Faraday Soc.,* **50,** 881 (1954).
7. W. Kuhn and F. Grun, *Kolloid-Z.,* **101,** 248 (1942).
8. W. Kuhn and H. Kuhn, *Helv. Chim. Acta,* **29,** 1095 (1946).
9. A. Isihara, N. Hashitsume, and M. Tatibana, *J. Chem. Phys.,* **18,** 108 (1951).
10. M. C. Wang and E. Guth, *J. Chem. Phys.,* **20,** 1144 (1952).
11. L. R. G. Treloar, *Trans. Faraday Soc.,* **40,** 109 (1944).
12. L. R. G. Treloar, *Trans. Faraday Soc.,* **43,** 284 (1947).
13. D. W. Saunders, *Trans. Faraday Soc.,* **52,** 1414 (1956).
14. W. Kuhn and H. Kuhn, *Helv. Chim. Acta,* **26,** 434 (1943).
15. L. Mullins and W. F. Watson, *J. Appl. Polymer Sci.,* **1,** 245 (1959).

Synopsis

Departures from behavior predicted by the statistical theory of rubberlike elasticity, which occur at high extensions, are ascribed to the finite extensibility of network chains. By use of a non-Gaussian statistical theory, a relation is obtained between the extension ratio λ^*, the extension at which departures are small but significant and the degree of crosslinking. Experimental results on the dependence of λ^* on the degree of crosslinking and on the degree of swelling are in good agreement with theoretical predictions. It is shown that the additional determination of λ^* permits the calculation of both the degree of crosslinking and the extent of network flaws due to chain ends, from a single simple extension stress–strain curve. The calculation of these two basic parameters has hitherto been unattainable from measurements on vulcanized rubbers alone. This development provides a new technique of particular value in studies of the degradation of vulcanized networks.

Résumé

Les déviations des prédictions de la théorie statistique de l'élasticité caoutchouteuse, qui se présentent à haute extension, sont attribuées à l'extensibilité limitée des chaînes du réseau. Avec la théorie statistique non-gaussienne on obtient une relation entre le rapport d'extension λ^*, l'extension à laquelle des écarts bien que faibles sont néanmoins significatifs, et le degré de pontage. Les résultats expérimentaux sur la dépendance de λ^* en fonction du degré de pontage et du degré de gonflement sont en bon accord avec les prévisions de la théorie. On a montré que la détermination additionnelle de λ^* permet le calcul du degré de pontage ainsi que l'extension des modifications réticulaires dues aux fins de chaîne, à partir d'une seule et simple courbe d'extension. Le calcul de ces deux paramètres de base a été toujours impossible à déterminer par des mesures sur le caoutchouc vulcanisé seul; et ce développement fournit une nouvelle technique de valeur particulière dans l'étude de la dégradation des réseaux vulcanisés.

Zusammenfassung

Abweichungen von den Voraussagen der statistischen Theorie der Kautschukelastizität, die bei hoher Dehnung auftreten, werden der begrenzten Dehnbarkeit der Netzketten zugeschrieben. Auf Grundlage einer nicht-Gaussschen statistischen Theorie wird eine Beziehung zwischen dem Dehnungsverhältnis λ^*, der Dehnung, bei welcher Abweichungen einen zwar kleinen aber charakteristischen Betrag besitzen, und dem Vernetzungsgrad erhalten. Die experimentellen Ergebnisse bezüglich der Abhängigkeit von λ^* von Vernetzungsgrad und vom Quellungsgrad stimmen gut mit den theoretischen Voraussagen überein. Es wird gezeigt, dass die zusätzliche Bestimmung von λ^* sowohl die Berechnung des Vernetzungsgrades als auch des Ausmasses des Fliessens des Netzwerkes das durch freie Kettenenden hervorgerufen wird aus der Spannungs-Dehnungskurve eines einzigen einfachen Dehnungsversuches gestattet. Die Berechnung dieser beiden grundlegenden Parameter war bisher aus Messungen an vulkanisiertem Kautschuk allein nicht durchführbar; die hier gegebene Entwicklung liefert eine neue Methode, die besonders für Untersuchungen über den Abbau von vernetzten Vulkanisaten wertvoll ist.